

Wind-modulated groundwater discharge along a microtidal Arctic coastline

Julia A. Guimond¹, Cansu Demir², Barret L. Kurylyk³, Michelle A. Walvoord⁴, James W. McClelland⁵, M. Bayani Cardenas²

¹Department of Applied Ocean Physics and Engineering, Woods Hole Oceanographic Institution, Woods Hole, MA, United States of America

²Department of Geological Sciences, The University of Texas at Austin, Austin, TX, United States of America

³Department of Civil and Resource Engineering and Centre for Water Resources Studies, Dalhousie University, Halifax, NS, Canada

⁴US Geological Survey, Earth System Processes Division, Denver, CO, United States of America

⁵Ecosystems Center, Marine Biological Laboratory, Woods Hole, MA United States of America

Email: julia.guimond@whoi.edu

Key words: Arctic, coastal groundwater, submarine groundwater discharge, cryohydrogeology, groundwater-surface water exchange

"This draft manuscript is distributed solely for purposes of scientific peer review. Its content is deliberative and predecisional, so it must not be disclosed or released by reviewers. Because the manuscript has not yet been approved for publication by the U.S. Geological Survey (USGS), it does not represent any official USGS finding or policy."

Abstract

Groundwater discharge transports dissolved constituents to the ocean, affecting coastal carbon budgets and water quality. However, the magnitude and mechanisms of groundwater exchange along rapidly transitioning Arctic coastlines are largely unknown due to limited observations. Here, using first-of-its-kind coastal Arctic groundwater timeseries data, we evaluate the magnitude and drivers of groundwater discharge to Alaska's Beaufort Sea coast. Darcy flux calculations reveal temporally variable groundwater fluxes, ranging from -6.5 cm/d (recharge) to 14.1 cm/d (discharge), with fluctuations in groundwater discharge or aquifer recharge over diurnal and multiday timescales. The average flux during the monitoring period of 4.9 cm/d is in line with previous estimates, but the maximum discharge exceeds previous estimates by over an order-of-magnitude. While the diurnal fluctuations are small due to the microtidal conditions, multiday variability is large and drives sustained periods of aquifer recharge and groundwater discharge. Results show that wind-driven lagoon water level changes are the dominant mechanism of fluctuations in land-sea hydraulic head gradients and, in turn, groundwater discharge. Given the microtidal conditions, low topographic relief, and limited rainfall along the Beaufort Sea coast, we identify wind as an important forcing mechanism of coastal groundwater discharge and aquifer recharge with implications for nearshore biogeochemistry. This study provides insights into groundwater flux dynamics along this coastline over time and highlights an oft overlooked discharge and circulation mechanism with implications towards refining solute export estimates to coastal Arctic waters.

1. Introduction

High-latitude coastlines are rapidly changing yet understudied due to difficult field conditions, limited points of coastal access, and short summer open-water periods. Much of the present understanding of northern coastal change is based on widely available observations by satellites. However, such spaceborne views do not capture any below-ground hydrologic processes. Few measurements of groundwater-ocean exchange exist in the Arctic, and those that do exist rely on data collected from only a few time points, making modulators of exchange difficult to identify and limiting spatiotemporal estimates of groundwater discharge (Connolly et al., 2020; Dimova et al., 2015). Given the role of groundwater as a major transport mechanism of terrestrial and permafrost thaw-mobilized carbon, nutrients, and contaminants to the nearshore ocean (e.g., Connolly et al., 2020), and as a potential catalyst of drastic changes experienced along Arctic coastlines (Fritz et al., 2017; Guimond et al., 2021; Irrgang et al., 2022; Lecher, 2017), this understanding is fundamental for assessments and projections of nearshore biogeochemical processes that influence marine productivity and ecosystems.

Coastal groundwater dynamics and exchange with the nearshore ocean are determined by the hydraulic head gradient between terrestrial water tables and sea surface level. The terrestrial water table elevation, influenced by aquifer recharge and nearshore topography, directly affects land-sea hydraulic gradients and fresh groundwater discharge to the ocean (Glover, 1959; Luijendijk et al., 2020). Closer to the coast, tidal sea-level fluctuations drive localized oscillations in aquifer hydraulic gradients and sea water circulation (i.e., tidal pumping), with tide-driven circulation and exchange directly related to tidal amplitude (Taniguchi, 2002; Wilson et al., 2015). Waves drive similar processes to tides but on much shorter time and spatial scales, and wave-driven impacts on groundwater scale with the wave height (Santos et al., 2012). While these processes influence groundwater dynamics globally, their relative importance, as well as other drivers/modulators of groundwater discharge, along Arctic coastlines are not well understood.

Arctic coastal aquifers are distinctive due to seasonally frozen conditions that limit periods of hydrological activity to the summer months. In high-latitude environments, groundwater flow is mediated by shallow aquifers formed by seasonal ground thaw (Walvoord & Kurylyk, 2016). Frozen-ground permeability is orders of magnitude lower than unfrozen ground (Burt &

Williams, 1976; McCauley et al., 2002), which causes shallow winter groundwater flow to cease. While permafrost acts as a largely impermeable lower boundary to groundwater flow, the seasonally variable supra-permafrost aquifer is a critical control on the magnitude of recharge, groundwater dynamics, and surface water-groundwater connectivity (Lamontagne-Hallé et al., 2018; Walvoord & Striegl, 2007). Sea ice also limits the period over which waves and tides interact with Arctic coastal tundra to the short open-water season.

More than half of the Beaufort Sea coast is fringed by shallow lagoons (< 7 m) that are confined by discontinuous barrier islands and where the tides are microtidal (Dunton et al., 2012). The shallow water and short fetch in the lagoons (< 4 m) limits wave height (Zimmermann et al., 2022). Thus, wave and tidal pumping are likely minor drivers of groundwater discharge. As a result, additional controls, such as wind and freezing-related processes, may play important roles in mediating coastal groundwater discharge and local circulation. Local and remote wind effects have been shown to exert a major control on surface water dynamics in shallow lagoons globally (Colvin et al., 2018; Garvine, 1985; Martin et al., 2004; Möller et al., 2001; Smith, 1990; Weaver et al., 2016). Remote winds on the continental shelf can influence sea level adjacent to an estuary or lagoon entrance due to Ekman transport and drive subsequent changes in lagoon level. Local winds can exert a stress directly on the sea surface, altering local currents and sea level (Wong & Valle-Levinson, 2002). Along the Beaufort Sea coast where westward longshore currents dominate, westerly (easterly) winds have been associated with high (low) sea surface levels (Arp et al., 2010; Reimnitz & Maurer, 1979). Previous work has linked these wind-driven sea-level changes with enhanced subterranean seawater circulation and vertical, offshore submarine groundwater discharge, particularly during high-wind events (George et al., 2020; Moore et al., 2022; Rodellas et al., 2020; Stieglitz et al., 2013; Swarzenski et al., 2017). However, the role of wind on lateral, nearshore groundwater discharge and circulation, and under non-event conditions has not been quantified, raising the question of the impact of wind on groundwater-surface water interactions along coastlines such as the Beaufort Sea with little tide- and wave-driven groundwater pumping.

The limited knowledge of Arctic coastal groundwater dynamics is based on fewer than a handful of studies that quantify groundwater discharge over relatively short, non-continuous sampling periods. One seminal study quantifying Arctic groundwater discharge (Dimova et al. 2015) used

a radon mass-balance approach to quantify integrated fresh and saline groundwater discharge to Elson Lagoon, Alaska. Groundwater discharge was estimated to be 1 cm/d during the open-water season. Given the microtidal environment and low aquifer hydraulic gradients due to the limited topography along the Beaufort Sea coast, Dimova et al. (2015) suggested that discharge was predominantly driven by wave setup and meltwater from a thawing supra-permafrost aquifer or from degrading permafrost. More recently, Connolly et al. (2020) identified groundwater as an important mechanism of carbon export along Alaska's north slope, with radon-based discharge estimates on the order of $42.6 \text{ m}^3/\text{d}/\text{m}$. They assumed that 1-5% of the measured discharge was due to land-derived freshwater fluxes given the low topographic gradients and limited tidal and wave pumping. These studies are valuable first estimates of groundwater discharge, yet the restricted temporal coverage limits mechanistic assessments of the drivers mediating coastal groundwater flow and variability with time.

In this study, we quantify and evaluate the modulators of coastal groundwater discharge along a low-lying Arctic coastline using newly collected coastal Arctic groundwater timeseries data that enable deeper exploration into the unique aspects of coastal groundwater discharge in high-latitude environments. Results point to wind as a key modulator of coastal Arctic groundwater discharge and porewater circulation and suggest that wind may be an overlooked driver of groundwater discharge globally.

2. Study Area

Field studies were conducted adjacent to Simpson Lagoon in Prudhoe Bay, Alaska along the central Beaufort Sea coast (70.508043°N , $-149.657897^\circ\text{W}$) (Figure 1a). Simpson Lagoon is a large, microtidal ($\sim 0.15 \text{ m}$ range) lagoon system confined by barrier islands with multiple connections to the ocean. Lagoons are present along over 50% of the Beaufort Sea coast, and thus, this site is representative of a majority of coastlines along the North Slope of Alaska but differs from coastlines that are exposed to the open ocean or higher in elevation. The lagoon is covered with ice approximately November through June with open water from July to October. The predominant wind direction is east (E, 60° - 120°) with occasional westerly (W) winds (240° - 300°) (Figure 1c). Wind data were retrieved from the NOAA's Prudhoe Bay buoy, approximately 40 km east of the field site (Station PRDA2, National Data Buoy Center). For the period without data, from September 7-12, 2022, wind speed and direction were retrieved from

Weather Underground for Prudhoe Bay, AK. Total precipitation in Prudhoe Bay during the study period from July 22, 2022 to October 1, 2022 was 0.07 m. The average beach depth to frozen ground based on manual probing was 0.84 m in July. The terrestrial environment adjacent to Simpson Lagoon is coastal tundra with degrading high center polygons, low topographic slope (0.3°) (Farquharson et al., 2018), and continuous permafrost (Jorgenson et al., 2008). The investigation site was chosen based on its proximity to degrading arctic tundra, as evidenced by vegetation mortality and polygon degradation, which is occurring along large swaths of coastline in the area.

3. Data and Methods

Surface water levels in Simpson Lagoon were measured with a conductivity, temperature, depth (CTD) logger (Solinst Levelogger 5 LTC, Canada) deployed from July 22, 2022 to October 1, 2022, measuring continuously at fifteen-minute intervals. During the same period, groundwater fluctuations were measured in five piezometers installed along a shore-perpendicular transect from the lagoon to 19.6 m inland (Figure S1) with a shallow pond approximately 2 m landward of the well furthest from the lagoon. Piezometer locations were chosen to span the transition zone between the lagoon and the degrading tundra. Piezometers were constructed of 0.03175 m diameter schedule 40 PVC with 0.20 m well screen length and were manually installed with a post driver to the maximum depth possible (i.e., intersection with the top of frozen ground; depth ranged from 0.4-0.7 m) to help ensure they do not go dry during the monitoring period. Piezometers were developed (cleaned of fine grains) by rotating, tapping, and purging several times following installation. Each piezometer was equipped with a CTD logger to continuously monitor groundwater level, temperature, and salinity every fifteen minutes. Water levels were corrected for barometric pressure collected from the NOAA buoy PRDA (National Data Buoy Center). Surface water levels were also corrected for the inverted barometer effect with 15-minute data between August 1, 2022 and September 29, 2022 following the equation:

$$h = \frac{\Delta P}{\rho g}$$

where ρ is water density (1,025.5 km/m³), g is gravitational acceleration (9.83 m/s² at 70.5°N), and ΔP is the difference between local and average atmospheric pressure (1012 mPa) (Erikson et al., 2020).

The relative piezometer locations were surveyed with a robotic laser total station (Trimble S5) with millimeter precision. Slug tests were conducted in three piezometers of different depths, and the hydraulic conductivity (K) was calculated with the Hvorslev (1951) equation. Groundwater discharge was calculated by Darcy's Law using the average of the highest and lowest hydraulic conductivity values measured with slug tests in the field and the hydraulic gradient between Well 1 and Well 5 (Figure 1e). The total discharge (recharge) was calculated by summing the positive (negative) groundwater flux per unit area per 15-minute interval.

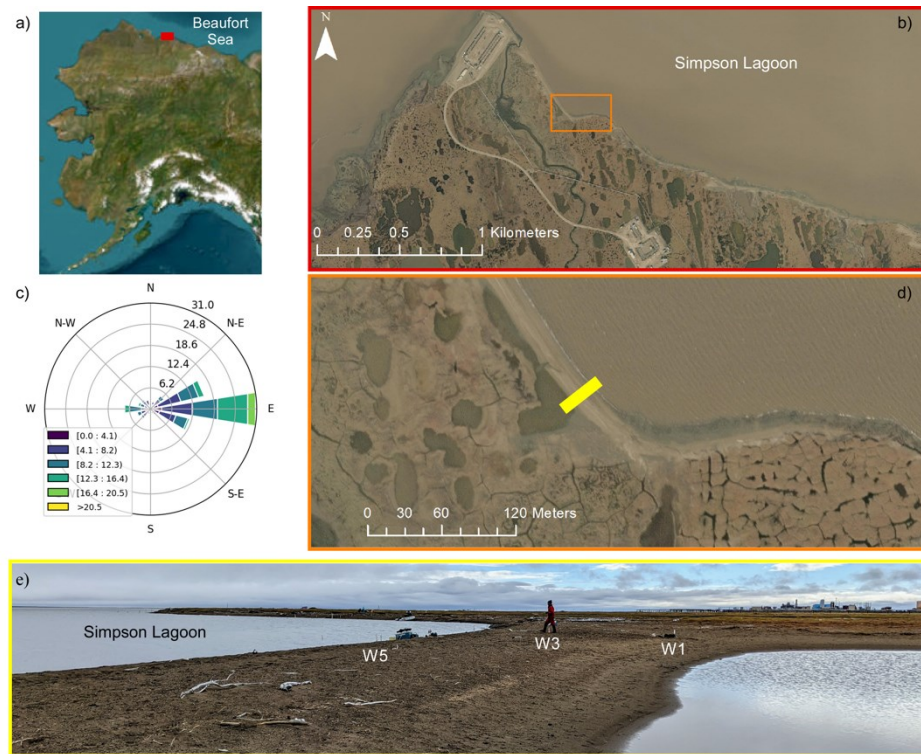


Figure 1. Field site information including a) general location map of Alaska, b) aerial image from red inset in a, c) wind rose for Prudhoe Bay, Alaska in units of m/s, d) aerial image of the well transect location (yellow) from the orange inset in b, and e) landscape photograph of site looking east from the yellow inset showing the lagoon, well (W1, W3, W5), and pond orientation. The wind rose in c) was created from the windrose Python package utilizing Matplotlib (Hunter, 2007) with 15-minute wind speed (m/s) and direction ($^{\circ}$) data from the NOAA buoy in Prudhoe Bay between 7/22/22 and 9/29/22. Data between 9/2/22 and 9/12/22 are blank due to logger failure. Imagery source ESRI.

To identify the relative role of different forcing mechanisms on groundwater dynamics (i.e., tides, precipitation, and wind), all surface and groundwater data, as well as wind direction and

predicted tide data, were run through a Fast Fourier Transform (FFT) conducted in Python on timeseries data between August 1, 2022 and September 29, 2022. Data between July 22-31, 2022

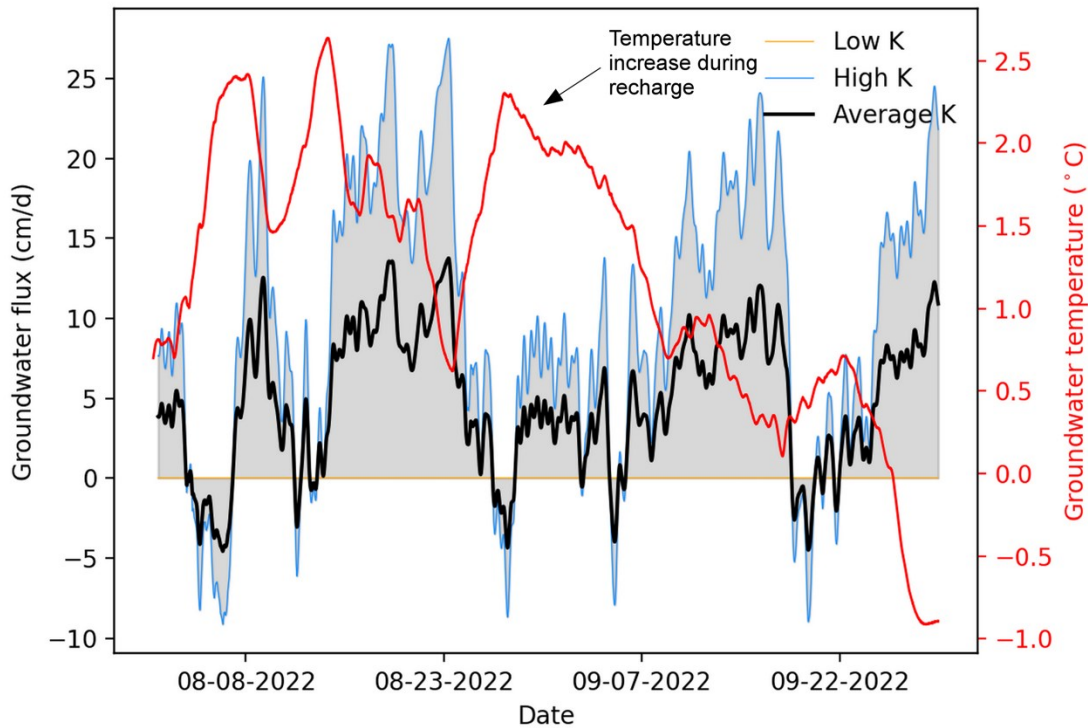


Figure 2. Eight-hour rolling mean groundwater flux along Simpson Lagoon where positive indicates discharge and negative indicates recharge, overlaid with groundwater temperature in the piezometer adjacent to the lagoon. Low K, high K, and average K indicate Darcy fluxes calculated with the low (0.06 cm/d), high (959 cm/d), and average (480 cm/d) hydraulic conductivity estimated with slug tests in the field.

were excluded due to erroneous values associated with water sample collection. The FFT on the lagoon, well, and predicted tides were based on 15-minute data. Predicted tide data were sourced from NOAA (Station 9497645, Prudhoe Bay, AK). For spectral analysis of wind direction, hourly wind data were used, where August 1, 2022 to September 9, 2022 and September 12-29, 2022 data were sourced from NOAA and data for September 2-12, 2022 were manually retrieved from Weather Underground (Prudhoe Bay, AK). The spectral amplitude was calculated by normalizing FFT results by the number of samples.

4. Results

Groundwater fluxes between August 1 and October 1, 2022 range from -6.5 cm/d (recharge) to 14.1 cm/d (discharge) with an average flux of 4.9 cm/d over the monitoring period (Figure 2) assuming an average K (480 cm/d). While the average flux is in line with Dimova et al. (2015),

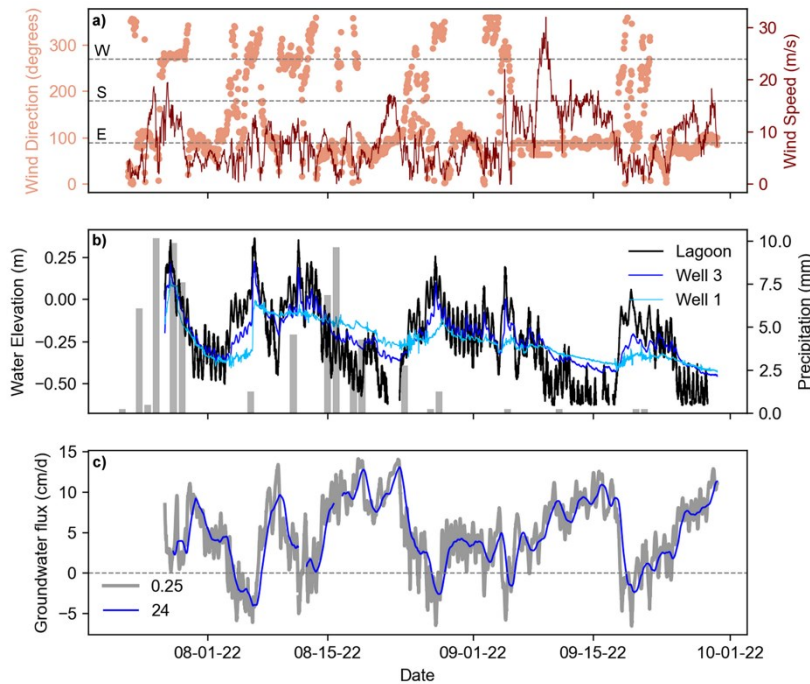


Figure 3. Time series data between July 27, 2022, and September 30, 2022, of a) wind speed and direction in Prudhoe Bay, Alaska, and b) Simpson Lagoon water level, groundwater levels in two wells, and precipitation (grey bars), and c) groundwater flux at 15-minute (0.25 hours) intervals (grey) and 24-hour rolling mean (blue).

certain periods exhibit discharge estimates that exceed previous estimates by over an order of magnitude. Our time series data capture large variability in groundwater flux magnitude and direction that could easily be undetected by short sampling campaigns and are not captured by integrative measures such as radon-based estimates (Figure 2). Tidal fluctuations in groundwater discharge were present but accounted for diurnal variability less than 5 cm/d due to the microtidal conditions in Simpson Lagoon. However, the range in groundwater fluxes exceeds 20 cm/d, with sustained periods of enhanced groundwater discharge (or discharge cessation) for multiple days that suggest additional discharge mechanisms (Figure 2). Below we discuss drivers of surface water (4.1) and groundwater (4.2) variability that result in fluctuations in hydraulic head gradients and groundwater exchange between land and sea along Alaska's North Slope.

4.1 Drivers of lagoon level fluctuations and impacts on groundwater dynamics

The average tidal range in Prudhoe Bay, Alaska is 0.15 m, yet surface water levels in Simpson Lagoon ranged from -0.45 m to 0.64 m relative to the average lagoon level across our time series for a total range of 1.1 m, indicating additional mechanism(s) are driving surface water variations

(Figure 3b). Calculations of barometric pressure fluctuations reveal that barometric effects increased sea level by a maximum of 0.17 m and decreased sea level by as much as 0.19 m, with an average offset of -0.04 m. Tidal and barometric effects alone cannot explain observed surface water level fluctuations.

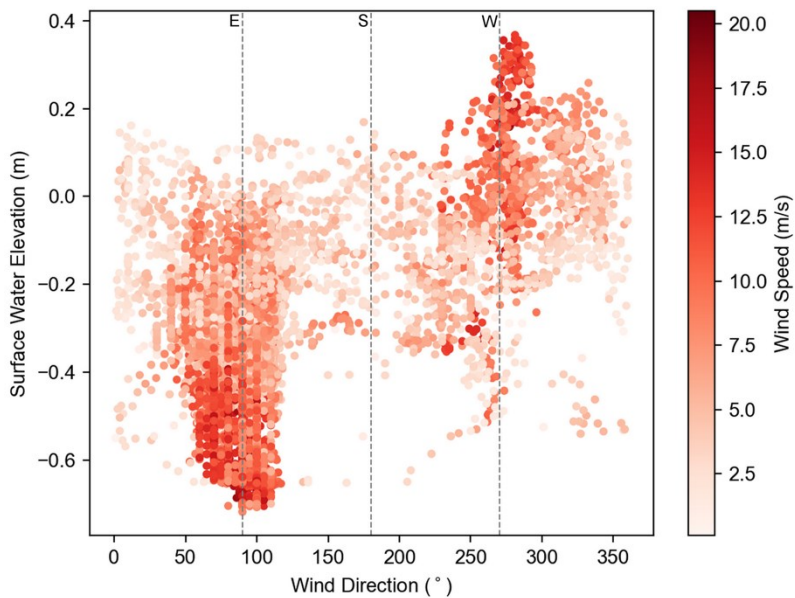


Figure 4. Scatter plot of Simpson Lagoon water level with wind direction. Colors indicate wind speed. Figure highlights low water levels during periods of ~easterly wind and high water levels during periods of ~westerly wind, particularly during periods with high wind speeds.

In addition to tides and barometric pressure, analyses reveal that wind strongly contributed to lagoon level variability. The correlation between wind direction and lagoon level shows high water events associated with wind between approximately 265°-295° (i.e., W), whereas low lagoon levels associated with winds between approximately 85°-115° (i.e., E) (Figure 4). The most extreme water levels (i.e., greatest set-up or set-down) are often associated with strong E or W wind events (Figure 3, 4). The large influence of wind on surface water level is further supported by FFT analyses. As expected, the FFT of the lagoon level time series shows peaks that correspond with the S2 (principal solar), M2 (principal lunar), K1 (principal lunar and solar), and O1 (principal lunar) tidal frequencies. Peaks also occur at lower frequencies, with periods

between 3-20 days (Figure 5b). These frequencies are not associated with tidal constituents but align with frequencies identified in the wind direction spectral analysis (Figure 5a).

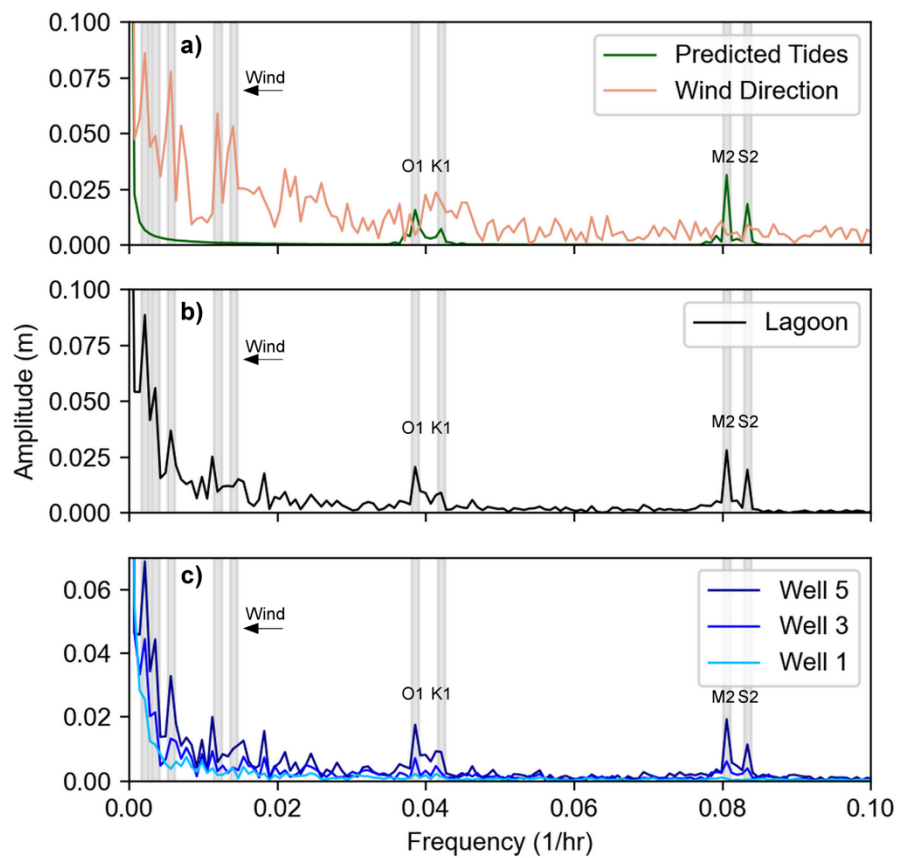


Figure 5. Spectral analyses for a) predicted tides and wind direction, b) lagoon level, and c) groundwater levels in three wells. Amplitude of wind direction in (a) divided by 250 in order to be plotted on the scale of predicted tides. S2, M2, K1, O1 tidal frequencies, and lower frequency peaks associated with wind are indicated with grey shading.

Wind-driven changes in surface water levels alter land-sea hydraulic gradients and drive sustained periods of groundwater discharge and active layer recharge that coincide with E and W winds, respectively, and that exceed tidally modulated groundwater fluxes (Figure 3c). The low lagoon levels during E winds increase the hydraulic gradient between the tundra and Simpson Lagoon, increasing the groundwater flux to the lagoon. Conversely, periods of high lagoon levels associated with W winds reverse the hydraulic gradient and drive surface water laterally into the supra-permafrost aquifer, while also driving recharge vertically through inundation. In addition to diurnal fluctuations in hydraulic gradients that occur in tidally dominated environments (Robinson et al., 2006), along Simpson Lagoon, enhanced groundwater discharge was

maintained for multiple days during E winds. For example, from August 13-26, 2022, and from September 5-18, 2022, only groundwater discharge occurred (Figure 2, 3). During high-water periods associated with W winds, groundwater discharge ceased, and aquifer recharge was maintained. For example, from August 3-7, 2022, only recharge into the coastal aquifer occurred (Figure 2).

These data are further supported by groundwater temperature measured in the wells. During our study period, the lagoon was warmer than the groundwater until September 25, 2022. Thus, during periods of recharge (negative fluxes), the groundwater temperature increased, suggesting heat advection from the influx of surface water into the active layer rather than just the propagation of a pressure wave (Figure 2).

4.2 Drivers of terrestrial water table changes

The influence of sea-level variability was observed in groundwater levels of all monitoring wells, with the magnitude of influence decreasing as expected with distance from the lagoon (Figure 3c; Figure S2). Near the lagoon (Well 5), the range in groundwater level was 0.97 m, with fluctuations in line with both tidal and wind-driven frequencies. Spectral analyses show that while the tidal constituents were apparent, the largest groundwater fluctuations occurred at periods ≥ 3.5 days, with peaks in line with frequencies associated with wind direction changes (Figure 5a,c). At the well farthest from the lagoon (Well 1), the range in water level between July and October was 0.42 m. The largest fluctuations were associated with W wind events and the highest lagoon water levels that overtopped the ground surface and recharged the aquifer (Figure 3b). As a result, heads in the well farthest from the lagoon remained elevated even after floodwaters receded, resulting in a larger hydraulic head gradient following westerly storm events.

A strong direct effect of precipitation on groundwater levels and land-sea hydraulic head gradients was not observed during most of the study period, as evidenced by minimal water table response to minor precipitation events (Figure 3b). A notable exception was a storm on July 27-28, 2022 that brought 17.5 mm of rain to the study area. Groundwater levels in all wells rose immediately following this storm event. However, this rain coincided with westerly wind which also increased water levels in the lagoon, making responses to high sea levels and to the storm event difficult to parse and minimizing changes in hydraulic head gradients. A second rain event

was observed on August 15-16, 2022 that was not associated with high lagoon levels. The perturbation to groundwater levels was small and did not result in a large change in the hydraulic head gradient.

5. Discussion

Groundwater discharge calculated from hydraulic head gradients and K estimates along Simpson Lagoon show wind-driven variability in groundwater discharge that exceeds tidal effects. We propose that wind-driven pumping – the recharge and discharge of coastal aquifers in response to wind-driven changes in hydraulic head gradients – is an important mechanism of groundwater discharge along Simpson Lagoon. Given the combination of relatively low topographic relief of coastal watersheds that limits the terrestrially-derived, fresh groundwater discharge, and low tidal range and wave amplitude that limits tidal and wave pumping, we suggest that wind-driven pumping is a dominant modulator of land-sea hydraulic gradients, which in turn controls the timing of aquifer recharge and groundwater discharge along the Beaufort Sea coast. It is important to note that flux estimates capture total lateral groundwater flow, including fresh, terrestrial-based water as well as recharged lagoon water.

While the amplitude of lagoon level fluctuations associated with wind events are in line with tidal oscillations in macrotidal systems, the timescales of fluctuations are unique and variable. In contrast to the sub-daily timescales of tidal and wave pumping, wind-driven pumping acts over multiday periods, resulting in sustained periods of aquifer recharge or groundwater discharge, with potential implications for biogeochemical cycling and solute export. Previous work along Alaska's North Slope estimated that terrestrially derived groundwater fluxes are a relatively small fraction (1-5%) of total groundwater discharge given the flat topography of the surrounding region and low tidal range. When combined with porewater dissolved organic carbon concentrations, Connolly et al. (2020) estimated a terrestrially-derived groundwater organic carbon export of 14-71 kg C/km/d. However, these estimates do not consider the additional circulation and export due to wind-driven pumping. Tide-driven coastal groundwater discharge and circulation often have short residence times, limiting biogeochemical reactions that can occur from surface water and groundwater mixing. With sustained recharge/discharge, the groundwater pumping driven by wind-driven surface water level changes may facilitate longer, sustained reactions. The lower frequencies of wind pumping, compared to frequencies of

waves or diurnal tides, drives water table fluctuations and associated mixing further inland because the signal propagation is directly linked to its period (e.g., Eq. 9 of Nielsen, 1990). During high water associated with W wind, oxygen-rich lagoon water recharges the coastal supra-permafrost aquifer, interacting with the coastal sediments and organic matter. Recent work has shown that both shallow and deep tundra sediments have the potential to leach large concentrations of organic carbon into the porewater for potential mobilization to surface water reservoirs (Connolly et al., 2020). Given the high leaching potential of both shallow and deep sediment, the introduction of oxygen-rich water into the subsurface, and extended periods of sediment-water interactions, the recharged groundwater may become concentrated in organic matter and subsequently exported to the lagoon upon the next set-down period (E wind). Furthermore, the extended periods of enhanced discharge have the potential to drain deeper, older groundwater reservoirs with elevated organic matter concentrations due to the long residence times. Thus, we postulate that the terrestrially derived export of water and dissolved carbon to the coastal ocean may be even greater than previous estimates (i.e., Connolly et al., 2020). (Hu et al., 2006; McKenzie et al., 2021)

Considering discharge per unit area (m^2), the total groundwater discharge between August 1 and September 29 is $3.12 \text{ m}^3/\text{m}^2$ and total recharge is $-0.22 \text{ m}^3/\text{m}^2$, with average daily values of $0.05 \text{ m}^3/\text{m}^2\text{d}$ and $-0.004 \text{ m}^3/\text{m}^2\text{d}$, respectively. Assuming a lagoon coastline of 546 km along Alaska's North Slope (Jorgenson & Brown, 2005), we estimate $1.58 \times 10^6 \text{ m}^3/\text{m}$ of local and circulated coastal groundwater is discharged to Beaufort lagoons during the study period. This estimate is only for a unit area and does not integrate over the seepage zone, along which flux varies, and thus, more than $1.58 \times 10^6 \text{ m}^3/\text{m}$ of local and circulated coastal groundwater could be discharged. Assuming a concentration of 33.2 mg/L of groundwater dissolved organic carbon (Connolly et al., 2020), we estimate a flux of $5.2 \times 10^5 \text{ kg C}$ to the lagoon during the monitoring period.

It is important to note that the monitoring period in this study did not capture any storm events, which have been shown to substantially increase groundwater discharge (Hu et al., 2006; McKenzie et al., 2021). Thus, groundwater discharge and associated solutes to the coastal Arctic may be even greater than estimated in this study. More data collection is needed over longer timescales that capture storm events and shoulder seasons to both assess storm influences on Arctic coastal groundwater discharge and confine annual discharge estimates. It is also important

to note that Darcy flux calculations have inherent uncertainty, particularly associated with estimates of hydraulic conductivity. Future work should incorporate multiple methodological approaches for groundwater discharge quantification where feasible to help limit estimate uncertainty.

Permafrost is present along over 34% of the global coastline (Lantuit et al., 2012), making understanding groundwater dynamics and exchange with Arctic coastal waters critically important for present-day assessments of ecosystem function and projections with climate change in a rapidly evolving Arctic. Erosion has been long identified as a mechanism of carbon release to the continental shelf and atmosphere (Jorgenson & Brown, 2005; Terhaar et al., 2021; Vonk et al., 2012), yet with hydrogeological activation and sea ice loss, in combination with the high sediment and porewater carbon concentrations in the Arctic (Connolly et al., 2020; Schuur et al., 2015; Turetsky et al., 2019), groundwater may become an increasingly important conduit of carbon to coastal waters (Connolly et al., 2020). Furthermore, some climate model projections point to stronger winds in a future Arctic with less sea ice (Mioduszewski et al., 2018; Vavrus & Alkama, 2022), suggesting that wind-driven coastal groundwater exchange may be an increasingly important driver of groundwater discharge and terrestrial carbon export. In addition, intensifying coastal storms linked to warmer oceans and higher winds (IPCC, 2019) may drive more frequent and intensive coastal flooding and recharge of inundated seawater (Cantelon et al., 2022). This is a different, but related, wind-driven mechanism than the wind-driven set-up investigated in the present study, yet both mechanisms have the potential to recharge coastal tundra with seawater during westerly wind events, with potential implications for coastal permafrost (Guimond et al., 2021; Zhang et al., 2023) and land surface elevation (Tape et al., 2013) and may also have applications for coastlines subject to storm events.

6. Conclusion

Using newly acquired groundwater timeseries data, this study makes important advancements in understanding groundwater dynamics along Alaska's North Slope. We find that wind-driven pumping is a dominant modulator of coastal groundwater dynamics and exchange with the coastal ocean, exceeding the impact of both tides and precipitation on groundwater flow. Given the sustained periods of recharge and discharge due to wind direction, we postulate that

groundwater discharge may play an even greater role in lateral carbon export than previously estimated.

Acknowledgments

This work was funded by the National Science Foundation through grants NSF EAR-PF-1952627 to JG and ANS-1938820 to MBC and JM. It was also supported by the Beaufort Lagoon Ecosystems Long Term Ecological Research program (NSF-PLR-1656026). There are no competing financial, professional or personal interests.

Data availability statement

Upon manuscript acceptance, the data collected and used in this study will be published at the Environmental Data Initiative (EDI) with a DOI and made publicly available through both the EDI and Beaufort Lagoon Ecosystems LTER data portals.

References

Arp, C. D., Jones, B. M., Schmutz, J. A., Urban, F. E., & Jorgenson, M. T. (2010). Two mechanisms of aquatic and terrestrial habitat change along an Alaskan Arctic coastline. *Polar Biology*, 33(12), 1629–1640. <https://doi.org/10.1007/s00300-010-0800-5>

Burt, T. P., & Williams, P. J. (1976). Hydraulic conductivity in frozen soils. *Earth Surface Processes, 1*(4), 349–360. <https://doi.org/10.1002/esp.3290010404>

Cantelon, J. A., Guimond, J. A., Robinson, C. E., Michael, H. A., & Kurylyk, B. L. (2022). Vertical Saltwater Intrusion in Coastal Aquifers Driven by Episodic Flooding: A Review. *Water Resources Research*, 58(11), e2022WR032614. <https://doi.org/10.1029/2022WR032614>

Colvin, J., Lazarus, S., Split, M., Weaver, R., & Taeb, P. (2018). Wind driven setup in east central Florida's Indian River Lagoon: Forcings and parameterizations. *Estuarine, Coastal and Shelf Science*, 213, 40–48. <https://doi.org/10.1016/j.ecss.2018.08.004>

Connolly, C. T., Cardenas, M. B., Burkart, G. A., Spencer, R. G. M., & McClelland, J. W. (2020). Groundwater as a major source of dissolved organic matter to Arctic coastal waters. *Nature Communications*, 11(1), Article 1. <https://doi.org/10.1038/s41467-020-15250-8>

Dimova, N. T., Paytan, A., Kessler, J. D., Sparrow, K. J., Garcia-Tigreros Kodovska, F., Lecher, A. L., Murray, J., & Tulaczyk, S. M. (2015). Current Magnitude and Mechanisms of Groundwater Discharge in the Arctic: Case Study from Alaska. *Environmental Science & Technology*, 49(20), 12036–12043. <https://doi.org/10.1021/acs.est.5b02215>

Dunton, K. H., Schonberg, S. V., & Cooper, L. W. (2012). Food Web Structure of the Alaskan Nearshore Shelf and Estuarine Lagoons of the Beaufort Sea. *Estuaries and Coasts*, 35(2), 416–435. <https://doi.org/10.1007/s12237-012-9475-1>

Erikson, L. H., Gibbs, A. E., Richmond, B. M., Storlazzi, C. D., Jones, B. M., & Ohman, K. (2020). Changing storm conditions in response to projected 21st century climate change and the potential impact on an arctic barrier island–lagoon system—A pilot study for Arey Island and Lagoon, eastern Arctic Alaska. In *Changing storm conditions in response to projected 21st century climate change and the potential impact on an arctic barrier island–lagoon system—A pilot study for Arey Island and Lagoon, eastern Arctic Alaska* (USGS Numbered Series 2020–1142; Open-File Report, Vols. 2020–1142). U.S. Geological Survey. <https://doi.org/10.3133/of20201142>

Farquharson, L. M., Mann, D. H., Swanson, D. K., Jones, B. M., Buzard, R. M., & Jordan, J. W. (2018). Temporal and spatial variability in coastline response to declining sea-ice in northwest Alaska. *Marine Geology*, 404, 71–83. <https://doi.org/10.1016/j.margeo.2018.07.007>

Fritz, M., Vonk, J. E., & Lantuit, H. (2017). Collapsing Arctic coastlines. *Nature Climate Change*, 7(1), 6–7. <https://doi.org/10.1038/nclimate3188>

Garvine, R. W. (1985). A simple model of estuarine subtidal fluctuations forced by local and remote wind stress. *Journal of Geophysical Research: Oceans*, 90(C6), 11945–11948. <https://doi.org/10.1029/JC090iC06p11945>

George, C., Moore, W. S., White, S. M., Smoak, E., Joye, S. B., Leier, A., & Wilson, A. M. (2020). A New Mechanism for Submarine Groundwater Discharge From Continental Shelves. *Water Resources Research*, 56(11), e2019WR026866. <https://doi.org/10.1029/2019WR026866>

Glover, R. E. (1959). The pattern of fresh-water flow in a coastal aquifer. *Journal of Geophysical Research*, 64(4), 457–459. <https://doi.org/10.1029/JZ064i004p00457>

Guimond, J. A., Mohammed, A. A., Walvoord, M. A., Bense, V. F., & Kurylyk, B. L. (2021). Saltwater Intrusion Intensifies Coastal Permafrost Thaw. *Geophysical Research Letters*, 48(19), 1–10. <https://doi.org/10.1029/2021GL094776>

Hu, C., Muller-Karger, F. E., & Swarzenski, P. W. (2006). Hurricanes, submarine groundwater discharge, and Florida's red tides. *Geophysical Research Letters*, 33(11). <https://doi.org/10.1029/2005GL025449>

Hvorslev, M. J. (1951). *Time Lag and Soil Permeability in Ground-water Observations*. Waterways Experiment Station, Corps of Engineers, U.S. Army.

IPCC, 2019: IPCC Special Report on the Ocean and Cryosphere in a Changing Climate [H.-O. Pörtner, D.C. Roberts, V. Masson-Delmotte, P. Zhai, M. Tignor, E. Poloczanska, K. Mintenbeck, A. Alegria, M. Nicolai, A. Okem, J. Petzold, B. Rama, N.M. Weyer (eds.)]. Cambridge University Press, Cambridge, UK and New York, NY, USA, 755 pp. <https://doi.org/10.1017/9781009157964>.

Irrgang, A. M., Bendixen, M., Farquharson, L. M., Baranskaya, A. V., Erikson, L. H., Gibbs, A. E., Ogorodov, S. A., Overduin, P. P., Lantuit, H., Grigoriev, M. N., & Jones, B. M. (2022). Drivers, dynamics and impacts of changing Arctic coasts. *Nature Reviews Earth & Environment*, 3(1), 39–54. <https://doi.org/10.1038/s43017-021-00232-1>

Jorgenson, M. T., & Brown, J. (2005). Classification of the Alaskan Beaufort Sea Coast and estimation of carbon and sediment inputs from coastal erosion. *Geo-Marine Letters*, 25(2–3), 69–80. <https://doi.org/10.1007/s00367-004-0188-8>

Jorgenson, M., Yoshikawa, K., Kanevskiy, M., Shur, Y., Romanovsky, V., Marchenko, S., & Jones, B. (2008). *Permafrost Characteristics of Alaska + Map*.

Lamontagne-Hallé, P., McKenzie, J. M., Kurylyk, B. L., & Zipper, S. C. (2018). Changing groundwater discharge dynamics in permafrost regions. *Environmental Research Letters*, 13(8), 084017. <https://doi.org/10.1088/1748-9326/aad404>

Lantuit, H., Overduin, P. P., Couture, N., Wetterich, S., Aré, F., Atkinson, D., Brown, J., Cherkashov, G., Drozdov, D., Donald Forbes, L., Graves-Gaylord, A., Grigoriev, M., Hubberten, H. W., Jordan, J., Jorgenson, T., Ødegård, R. S., Ogorodov, S., Pollard, W. H., Rachold, V., ... Vasiliev, A. (2012). The Arctic Coastal Dynamics Database: A New Classification Scheme and Statistics on Arctic Permafrost Coastlines. *Estuaries and Coasts*, 35(2), 383–400. <https://doi.org/10.1007/s12237-010-9362-6>

Lecher, A. (2017). Groundwater Discharge in the Arctic: A Review of Studies and Implications for Biogeochemistry. *Hydrology*, 4(3), 41. <https://doi.org/10.3390/hydrology4030041>

Luijendijk, E., Gleeson, T., & Moosdorf, N. (2020). Fresh groundwater discharge insignificant for the world's oceans but important for coastal ecosystems. *Nature Communications*, 11(1). <https://doi.org/10.1038/s41467-020-15064-8>

Martin, J. B., Cable, J. E., Swarzenski, P. W., & Lindenbergh, M. K. (2004). Enhanced Submarine Ground Water Discharge from Mixing of Pore Water and Estuarine Water. *Groundwater*, 42(7), 1000–1010. <https://doi.org/10.1111/j.1745-6584.2004.tb02639.x>

McCauley, C. A., White, D. M., Lilly, M. R., & Nyman, D. M. (2002). A comparison of hydraulic conductivities, permeabilities and infiltration rates in frozen and unfrozen soils. *Cold Regions Science and Technology*, 34(2), 117–125. [https://doi.org/10.1016/S0165-232X\(01\)00064-7](https://doi.org/10.1016/S0165-232X(01)00064-7)

McKenzie, T., Dulai, H., & Fuleky, P. (2021). Traditional and novel time-series approaches reveal submarine groundwater discharge dynamics under baseline and extreme event conditions. *Scientific Reports*, 11(1), 22570. <https://doi.org/10.1038/s41598-021-01920-0>

Mioduszewski, J., Vavrus, S., & Wang, M. (2018). Diminishing Arctic Sea Ice Promotes Stronger Surface Winds. *Journal of Climate*, 31(19), 8101–8119. <https://doi.org/10.1175/JCLI-D-18-0109.1>

Möller, O. O., Castaing, P., Salomon, J.-C., & Lazure, P. (2001). The influence of local and non-local forcing effects on the subtidal circulation of Patos Lagoon. *Estuaries*, 24(2), 297–311. <https://doi.org/10.2307/1352953>

Moore, W. S., Vincent, J., Pickney, J. L., & Wilson, A. M. (2022). Predicted Episode of Submarine Groundwater Discharge Onto the South Carolina, USA, Continental Shelf and Its Effect on Dissolved Oxygen. *Geophysical Research Letters*, 49(24), e2022GL100438. <https://doi.org/10.1029/2022GL100438>

Nielsen, P. (1990). Tidal dynamics of the water table in beaches. *Water Resources Research*, 26(9), 2127–2134. <https://doi.org/10.1029/WR026i009p02127>

Reimnitz, E., & Maurer, D. K. (1979). Effects of Storm Surges on the Beaufort Sea Coast, Northern Alaska. *Arctic*, 32(4), 329–344.

Robinson, C., Gibbes, B., & Li, L. (2006). Driving mechanisms for groundwater flow and salt transport in a subterranean estuary. *Geophysical Research Letters*, 33(3). <https://doi.org/10.1029/2005GL025247>

Rodellas, V., Cook, P. G., McCallum, J., Andrisoa, A., Meulé, S., & Stieglitz, T. C. (2020). Temporal variations in porewater fluxes to a coastal lagoon driven by wind waves and changes in lagoon water depths. *Journal of Hydrology*, 581, 124363. <https://doi.org/10.1016/j.jhydrol.2019.124363>

Santos, I. R., Eyre, B. D., & Huettel, M. (2012). The driving forces of porewater and groundwater flow in permeable coastal sediments: A review. *Estuarine, Coastal and Shelf Science*, 98, 1–15. <https://doi.org/10.1016/j.ecss.2011.10.024>

Schuur, E. A. G., McGuire, A. D., Schädel, C., Grosse, G., Harden, J. W., Hayes, D. J., Hugelius, G., Koven, C. D., Kuhry, P., Lawrence, D. M., Natali, S. M., Olefeldt, D., Romanovsky, V. E., Schaefer, K., Turetsky, M. R., Treat, C. C., & Vonk, J. E. (2015). Climate change and the permafrost carbon feedback. *Nature*, 520(7546), 171–179. <https://doi.org/10.1038/nature14338>

Smith, N. P. (1990). Computer simulation of tide-induced residual transport in a coastal lagoon. *Journal of Geophysical Research: Oceans*, 95(C10), 18205–18211. <https://doi.org/10.1029/JC095iC10p18205>

Stieglitz, T. C., van Beek, P., Souhaut, M., & Cook, P. G. (2013). Karstic groundwater discharge and seawater recirculation through sediments in shallow coastal Mediterranean lagoons, determined from water, salt and radon budgets. *Marine Chemistry*, 156, 73–84. <https://doi.org/10.1016/j.marchem.2013.05.005>

Swarzenski, P. W., Dulai, H., Kroeger, K. D., Smith, C. G., Dimova, N., Storlazzi, C. D., Prouty, N. G., Gingerich, S. B., & Glenn, C. R. (2017). Observations of nearshore groundwater discharge: Kahekili Beach Park submarine springs, Maui, Hawaii. *Journal of Hydrology: Regional Studies*, 11, 147–165. <https://doi.org/10.1016/j.ejrh.2015.12.056>

Taniguchi, M. (2002). Tidal effects on submarine groundwater discharge into the ocean. *Geophysical Research Letters*, 29(12), 2-1-2–3. <https://doi.org/10.1029/2002GL014987>

Tape, K. D., Flint, P. L., Meixell, B. W., & Gaglioti, B. V. (2013). Inundation, sedimentation, and subsidence creates goose habitat along the Arctic coast of Alaska. *Environmental Research Letters*, 8(4), 045031. <https://doi.org/10.1088/1748-9326/8/4/045031>

Terhaar, J., Lauerwald, R., Regnier, P., Gruber, N., & Bopp, L. (2021). Around one third of current Arctic Ocean primary production sustained by rivers and coastal erosion. *Nature Communications*, 12(1), 169. <https://doi.org/10.1038/s41467-020-20470-z>

Turetsky, M. R., Abbott, B. W., Jones, M. C., Walter Anthony, K., Olefeldt, D., Schuur, E. A. G., Koven, C., McGuire, A. D., Grosse, G., Kuhry, P., Hugelius, G., Lawrence, D. M., Gibson, C., & Sannel, A. B. K. (2019). Permafrost collapse is accelerating carbon release. *Nature*, 569(7754), 32–34. <https://doi.org/10.1038/d41586-019-01313-4>

Vavrus, S. J., & Alkama, R. (2022). Future trends of arctic surface wind speeds and their relationship with sea ice in CMIP5 climate model simulations. *Climate Dynamics*, 59(5), 1833–1848. <https://doi.org/10.1007/s00382-021-06071-6>

Vonk, J. E., Sanchez-Garcia, L., Van Dongen, B. E., Alling, V., Kosmach, D., Charkin, A., Semiletov, I. P., Dudarev, O. V., Shakhova, N., Roos, P., Eglinton, T. I., Andersson, A., & Gustafsson, A. (2012). Activation of old carbon by erosion of coastal and subsea permafrost in Arctic Siberia. *Nature*, 489(7414), 137–140. <https://doi.org/10.1038/nature11392>

Walvoord, M. A., & Kurylyk, B. L. (2016). Hydrologic Impacts of Thawing Permafrost-A Review. *Vadose Zone Journal*, 15(6), vzb2016.01.0010. <https://doi.org/10.2136/vzj2016.01.0010>

Walvoord, M. A., & Striegl, R. G. (2007). Increased groundwater to stream discharge from permafrost thawing in the Yukon River basin: Potential impacts on lateral export of carbon and nitrogen. *Geophysical Research Letters*, 34(12), L12402. <https://doi.org/10.1029/2007GL030216>

Weaver, R. J., Taeb, P., Lazarus, S., Splitt, M., Holman, B. P., & Colvin, J. (2016). Sensitivity of modeled estuarine circulation to spatial and temporal resolution of input meteorological forcing of a cold frontal passage. *Estuarine, Coastal and Shelf Science*, 183, 28–40. <https://doi.org/10.1016/j.ecss.2016.10.014>

Wilson, A. M., Evans, T. B., Moore, W. S., Schutte, C. A., & Joye, S. B. (2015). What time scales are important for monitoring tidally influenced submarine groundwater discharge? Insights from a salt marsh. *Water Resources Research*, 51(6), 4198–4207. <https://doi.org/10.1002/2014WR015984>

Wong, K-C, W., & Valle-Levinson, A. (2002). On the relative importance of the remote and local wind effects on the subtidal exchange at the entrance to the Chesapeake Bay. *Journal of Marine Research*, 60, 477–498. <https://doi.org/10.1357/002224002762231188>

Zhang, Y., Jafarov, E., Piliouras, A., Jones, B. M., Rowland, J., & Moulton, D. (2023). The thermal response of permafrost to coastal floodplain flooding. *Environmental Research Letters*. <https://doi.org/10.1088/1748-9326/acba32>

Zimmermann, M., Erikson, L. H., Gibbs, A. E., Prescott, M. M., Escarzaga, S. M., Tweedie, C. E., Kasper, J. L., & Duvoy, P. X. (2022). Nearshore bathymetric changes along the Alaska Beaufort Sea coast and possible physical drivers. *Continental Shelf Research*, 242, 104745. <https://doi.org/10.1016/j.csr.2022.104745>